N-80156

[redacted]

N65-82320
(ACCESSION NUMBER)

39
(PAGES)

CR 60961
(NASA CR OR TMX OR AD NUMBER)

(THRU)

None
(CODE)

(CATEGORY)

FACILITY FORM 602

JET PROPULSION LABORATORY
CALIFORNIA INSTITUTE OF TECHNOLOGY
PASADENA 3, CALIFORNIA

7

National Aeronautics and Space Administration
Contract No. NASw-6

Technical Release No. 34-26

# EVALUATION OF PIONEER IV ORBIT-DETERMINATION PROGRAM

M. Eimer
Y. Hiroshige

Copy No. 4

JET PROPULSION LABORATORY
A Research Facility of
National Aeronautics and Space Administration
Operated by
California Institute of Technology
Pasadena, California
February 22, 1960

## CONTENTS



## FIGURES

FIGURES (Cont'd)

# EVALUATION OF PIONEER IV ORBIT-DETERMINATION PROGRAM*

M. Eimer
Y. Hiroshige

Jet Propulsion Laboratory
California Institute of Technology
Pasadena, California

## I. INTRODUCTION

In December of 1958, and again in March of 1959, the NASA employed the JUNO II rocket system for the third and fourth attempts on the part of the U. S. to place a scientific payload on an escape trajectory in the vicinity of the Moon. The missile used in the December firing failed to achieve escape velocity, and the payload, PIONEER III, achieved a maximum distance from the center of the Earth of a little over 100, 000 km. The cosmic-ray data received from PIONEER III revealed the existence of a second Van Allen radiation belt at a higher altitude than that discovered by the satellite EXPLORER I.

The later attempt, the following March, was more successful. The payload PIONEER IV passed the Moon at a distance of approximately 60, 000 km and continued on to an interplanetary orbit with a period around the Sun of 395 days.

During the 80 hr of its battery life, this payload transmitted to Earth new information on the extent and nature of cosmic radiation in space, indicating

*This paper presents the results of one phase of research carried out at the Jet Propulsion Laboratory, California Institute of Technology, under Contract No. NASw-6, sponsored by the National Aeronautics and Space Administration.

variations on both the extent and intensity of the high altitude Van Allen radiation belt. Data were received to a range of 650,000 km.

Information on the position and speed of the probe and the telemetered scientific data were received and processed by a tracking and data handling network. The major requirements placed upon this network were:

1. To provide continuous reception of telemetering data to approximately 100,000 km from the Earth in order to receive cosmic-ray data from the outer radiation bands;
2. To provide at least intermittent reception of telemetering information to distances beyond the Moon;
3. To make precision angular measurements required for accurate determination of the flight paths of the probes.

A secondary objective was that the concepts and the basic hardware of the system could be utilized in the future evolution of a deep-space network which would meet the tracking, data handling, and computational requirements of more sophisticated deep-space experiments.

The deep-space tracking network being developed by the Jet Propulsion Laboratory (JPL) for the National Aeronautics and Space Administration (NASA) in cooperation with other countries around the world will make use of installations similar to those described in this paper. This network, and the elements of which it is composed, are being designed for the primary purpose of obtaining radioed data on position and telemetered measurements from lunar, interplanetary, and planetary flights.

## II. NETWORK CONFIGURATION

The primary data-acquisition and tracking network consisted of a set of receiving stations connected to a data-processing center by teletype and voice communications, and a number of cooperating tracking stations and computing centers. The primary net was established by the Jet Propulsion Laboratory and utilized (Fig. 1):

1. Tracking stations at the launch site at Cape Canaveral, Florida; at Mayaguez, Puerto Rico; and at Goldstone Lake, California.
2. A data-processing and computing center at Pasadena, California.
3. Message centers at Pasadena and Cape Canaveral.

The function of the launch-site station was to check out the payload radio equipment prior to launch and to provide telemetry reception and one-way doppler during the first 10 to 15 min of flight. This station utilized a narrow-band phase-locked receiver with a manually directed relatively broad beam antenna. For the PIONEER IV trajectory, the vehicle disappeared below the horizon 10 to 15 min after launching. Shortly before the time of loss at the launch site, approximately 6 min after lift-off, the vehicle appeared on the northwest horizon at the Puerto Rico station, and that station acquired the signal.

The Puerto Rico station has a narrow-band phase-locked receiver which is used in conjunction with a 10-ft-diameter automatic tracking antenna mounted on a modified Nike Az-El antenna pedestal (Fig. 2). Data provided by the station include vehicle coordinates (Az-El), one-way doppler, and telemetry.

After approximately 6 1/2 hr of tracking by the Puerto Rico station, the vehicle appeared on the southeast horizon at Goldstone Lake and that station acquired the signal (Fig. 3). At that time, the probe was approximately 80, 000 km from the Earth, still high in the sky at Puerto Rico, and providing a signal considerably above the threshold of the Puerto Rico station receiver.

The Goldstone station, which will be described in some detail, has a phase-locked receiver used in conjunction with an 85-ft-diameter polar-mounted tracking antenna. Basic data provided by the Goldstone installation are the same as provided by Puerto Rico: angular position, one-way doppler, and telemetry. The Goldstone station tracked the PIONEER probe from horizon to horizon, a period of about 9 hr. After the probe set in the west at Goldstone, it was not visible to that station for about 15 hr, after which time it was again acquired and tracked for another 9-hr period. This sequence was repeated for the life of the probe transmitter.

The tracking station coverage is shown pictorially in Fig. 4. Coverage by one of the major cooperating stations, the 250-ft-diameter Jodrell Bank radio telescope of the University of Manchester in England, is indicated on this drawing. A less artistic but more technically factual representation of the coverage by the network is shown in Fig. 5.

The doppler data from all stations and the angular information from the Puerto Rico and Goldstone stations, tagged with the exact Greenwich Mean Time, were automatically encoded into standard teletype format and transmitted to the Computing Center in California (Fig. 6). Automatic teletype to IBM-card converters were used to put the received data into the proper machine input format.

A sample of a data message received at the Computing Center from the Goldstone station is shown in Fig. 7. With machines adjusted for a transmission rate of 60 words/min, a single teletype line of data was transmitted in 7 sec. For use in the statistical evaluation of station performance after the completion of tracking, the comparatively high data-sampling rate of 6 samples/min was used throughout the PIONEER IV operation.

The Computing Center in Pasadena utilized primarily an IBM 704 computer. The computer results were monitored with several independent procedures using smaller electronic computers, desk calculators, and pre-computed charts. The IBM 704 computer at the Rand Corporation in Santa Monica, California, served as back-up. In the Computing Center the data were analyzed to provide rapid and precise acquisition pointing information for the tracking stations and accurate determination of the vehicle paths. The results of these computations were provided on IBM cards which were fed into a card-to-tape converter and transmitted to the appropriate tracking stations by teletype (Fig. 8).

The standard acquisition message provides data in 1-min intervals. For long-range predictions less frequent intervals were used. Figure 9 shows a sample of a standard message sent from the Computing Center to the Goldstone tracking station. The first four columns represent time, local hour angle, local declination angle, and counted doppler frequency in the same format and in the same coordinate system (including refraction corrections, etc.) as the expected data message. The remaining three columns represent local hour angle and local declination angle rates in thousandths of degrees per hour, and range in kilometers.

The flow of data into and out of the Computing Center was regulated from a communications net control center located in the computer area which directed the switching of communications lines actually carried out by the two message centers located on the east and west coasts of the United States.

The primary tracking network was thus an almost completely automatic system which, when receiving a probe signal, would automatically count, encode, transmit, and convert tracking data, and then compute, convert, transmit, and display acquisition data. The only nonautomatic function in the system was the carrying of data cards the 25 ft between converters and machine input and output.

## III. GOLDSTONE TRACKING STATION

A description of the Goldstone facility will illustrate the degree of complexity of the stations in the PIONEER III and IV network. Except for the larger antenna size and the greater permanency of the Goldstone station, the Puerto Rico and Goldstone installations are very similar. In particular, identical electronic equipment was installed at the two stations whenever feasible.

The Goldstone tracking antenna is 85 ft in diameter and is equatorially mounted. Significant parameters of the structure are:

1. Maximum tracking rate, 1 deg/sec in both axes

2. Maximum acceleration, 5 deg/sec$^2$
3. Accuracy of structure (constancy of axes alignment, etc.) on order of 1 min of arc.

The drive system has two speeds of operation: A high speed of 1 deg/sec for satellite tracking and a low speed capable of tracking the range which might be encountered with a space vehicle--0.1 to 0.005 deg/sec.

The feed for the 85-ft-diameter antenna was a simultaneous-lobing type, using four circularly polarized turnstile radiators located in front of a ground plane. The outputs of the individual radiators are combined in coaxial hybrids to derive the hour-angle and declination error patterns and the reference channel pattern. The electrical performance of the antenna is as follows:

1. Gain, 41 db above linearly polarized isotrope
2. Half-power beam width of reference channel, 0.9 to 1.3 deg

The radio receiver utilized with the 960-mc tracking system is a narrow-band phase-coherent double-conversion superheterodyne. It has three separate channels: a reference channel for detection of the carrier and telemetry signals and derivation of the coherent automatic gain control (AGC), and two similar error channels for the hour-angle and declination error signals from the simultaneous-lobing antenna. Parameters of the receiving systems can be adjusted to provide best performance for a particular mission. For the PIONEER IV tracking mission the significant characteristics of the receiver were:

1. Noise bandwidth at UHF, 20 cps
2. Noise temperature of receiver, 1330°K
3. Approximate receiver threshold, -154 dbm = 4 x $10^{-19}$ watts

For the above parameters, the maximum range for the PIONEER IV transmitter of 200-mw transmitted power was approximately $1.6 \times 10^6$ km for a unity S/N on the carrier signal and about 20-db S/N in the angle track and AGC loops. During the last phase of the PIONEER IV transmission, as the radiated power of the vehicle transmitter fell off because of depletion of the batteries, the bandwidth of the receiver was changed to a 10-cps value which increased the receiver sensitivity to about -157 dbm. This is equivalent to a range capability of $2.2 \times 10^6$ km for a 200-mw transmitted power.

## IV. DATA TRANSMISSION NETWORK

A communications system made up of voice and teletype facilities was established early in November 1958 to provide a reliable, rapid, and flexible means of transmission of digital data, technical information, and administrative messages between the various tracking stations, computing centers, and communications centers. This network provided full-time voice and 60-word/min teletype communication between stations at the Jet Propulsion Laboratory, the Goldstone Lake tracking station, and the Atlantic Missile Range by means of trunk tie-lines with existing administrative exchanges at these areas. The Mayaguez tracking station was linked to the net through the submarine cable which extends from Cape Canaveral to the southeastern range stations.

The over-all network, as illustrated in Fig. 10, provided for at least two half-duplex teletype circuits and two voice circuits between all points, with switching capabilities at the two message centers to provide for any makeup from a single point-to-point connection to a full party line.

## V. ANALYSIS OF THE TRACKING PROGRAM

The computing program was first constructed at the Jet Propulsion Laboratory for the tracking of PIONEER III. Although the December 1958 PIONEER III firing date was only 2 months after the acceptance at the Laboratory of an IBM 704 computer, the program used contained most of the essential principles. During the period between the firing of PIONEERS III and IV (less than 3 months), the method of combining data from the various sources and the methods of relative weighting of the data were significantly altered. The recently completed program, described in another report,[1] is the result of major re-organization of the computing procedure and incorporation of extensions in the types and quantity of data to be handled.

During the flight of PIONEER IV, the tracking program gave excellent results. The first 15 min of data after last-stage burnout were used to make pointing predictions for the Puerto Rico station for a time one hour later than the last data point used. These predictions and all later predictions for Puerto Rico were subsequently found to agree with the observations to within less than 0.2 deg. The initial conditions, obtained with 15 min of data, differ from the present best estimate by 12 km in injection altitude and 30 m/sec in velocity.

With 3 1/2 hours of data from Puerto Rico, an acquisition prediction was transmitted to the Goldstone station which agreed with subsequent observations

---

[1] Carr, R. E., and Hudson, H. R., The JPL Tracking and Orbit-Determination Program, Technical Release No. 34-7. Prepared for Seminar on Tracking Programs and Orbit Determination, Jet Propulsion Laboratory, February 22 - 26, 1960.

to within 0.1 deg. The initial conditions obtained at that time differ from the present best estimates by 2 km in altitude, 0.05 deg in latitude and longitude, 5 m/sec in velocity, and 0.1 deg in the velocity angles. All predictions made after the first day of tracking, for periods one day later, were found to agree with the observations to within 0.05 deg. At the distance of the Moon, the accuracy of the probe position as determined by the tracking and computation network was estimated to be 100 km.

The fundamental assumptions made in the design of the tracking program relate to the statistical properties of the errors in the data. It was assumed that (1) the errors in the data are normally distributed, (2) the errors are not correlated in time, (3) the errors in the two angular coordinates at a station are not correlated, and (4) bias is a constant over any sampling interval.

Figures 11 and 12 show the errors in actual samples of data with respect to the computed trajectory for the flight of PIONEER IV at ranges of 100,000 and 500,000 km, respectively. At close tracking ranges several characteristics of the tracking system are discernible (see Fig. 11). The declination-angle error graph clearly shows the sawtooth form with slopes proportional to the angular rates which are caused by roundoff in the digital encoding system. The hour-angle graph (Fig. 11) shows a sinusoidal form with a period of 25 min which, it was subsequently found, was caused by an out-of-round component in the angular readout system. At the larger ranges, the dominant feature of the error graphs is the indication of a substantial increase in noise in the system (see Fig. 12). It is evident that not all the fundamental assumptions as to the statistical nature of the tracking data were completely justified.

A. Methods of Analysis

An analysis of angular tracking data from the Goldstone station consisted of (1) separating noise from bias, (2) computing the root-mean-square error, (3) determining the noise autocorrelation functions, (4) computing the power spectral densities, (5) determining the form of the error-distribution function, and (6) determining the correlation between the errors in the declination and the hour angles.

Items (1) through (5) were computed for the declination angle using the IBM 704 computer routine developed by R. Mosher and R. Southworth[2] assuming that the data were stationary over 2-hour periods for the entire duration of the tracking period. The data were then analyzed in groups of 2-hour periods.

The one-dimensional distribution function is computed in the usual manner by counting the number of samples in each of the preselected intervals of width $1/2\,\sigma$, where $\sigma$ is the standard deviation from the mean, or

$$\sigma = \frac{1}{N}\left\{\sum_{i=1}^{N}\left[\Delta\delta_i - E(\Delta\delta_i)\right]^2\right\}^{1/2} \qquad (1)$$

where

$\Delta\delta_i \equiv$ residuals, or the difference between the observed declination angle and that obtained from the fitted trajectory.

[2] Auto-Correlation and Power Spectrum Analysis, NYCP2, 704 Program Library, SBC NY Data Processing Center (IBM), April 25, 1957.

The fitted trajectory is the best fit through all the data points in the least-mean-squares sense.

$E(\Delta\delta_i) \equiv$ average of the residuals

$N \equiv$ number of samples

The autocorrelation function, $R_p$, is computed from the following equation:

$$R_p = \frac{1}{N-p} \sum_{i=1}^{N-p} \left[\Delta\delta_i - E(\Delta\delta_i)\right]\left[\Delta\delta_{i+p} - E(\Delta\delta_i)\right] \qquad (2)$$

$$p = 0, 1, \ldots, M$$

where

$M \equiv$ number of lags.

The power spectrum, $L_h$, is computed from

$$L_h = \frac{2}{M}\left(R_0 + 2\sum_{p=1}^{M-1} R_p \cos\frac{\pi ph}{M} + R_m \cos \pi h\right) \qquad (3)$$

$$h = 0, 1, \ldots, M$$

The cross-correlation functions were computed for the residuals in the declination and the hour angles using the following equations:

$$R_{\Delta\alpha,\,\Delta\delta(p)} = \frac{1}{N-p}\sum_{i=1}^{N-p} \Delta\alpha_i\,\Delta\delta_{i+p} \qquad (4)$$

$$p = 0, 1, \ldots, M$$

$$R_{\Delta\delta,\ \Delta\alpha}(p) = \frac{1}{N - p} \sum_{i=1}^{N-p} \Delta\delta_i \ \Delta\alpha_{i+p} \tag{5}$$

$$p = 0, 1, \ldots, M$$

where

$\Delta\alpha_i \equiv$ residual in the local hour angle

$\Delta\delta_i \equiv$ residual in the declination angle

The number of samples, N, were taken over time periods greater than five hours.

A linear relationship between the residuals may be obtained by passing a straight line through the $\Delta\alpha$ - $\Delta\delta$ scatter diagram in the least-mean-square sense. Such a line is termed the "mean-square linear-regression line." In terms of normalized variables $(\xi_i, \eta_i)$, the regression line is

$$\eta_i = \rho\xi_i \tag{6}$$

where

$$\eta_i = \frac{\Delta\delta_i - E(\Delta\delta_i)}{\left[E(\Delta\delta_i^2) - E(\Delta\delta_i)^2\right]^{1/2}} \tag{7}$$

$$\xi_i = \frac{\Delta\alpha_i - E(\Delta\alpha_i)}{\left[E(\Delta\alpha_i^2) - E(\Delta\alpha_i)^2\right]^{1/2}} \tag{8}$$

$$\rho = \frac{E(\Delta\delta_i\ \Delta\alpha_i) - E(\Delta\delta_i)\ E(\Delta\alpha_i)}{\left[E(\Delta\alpha_i^2) - E(\Delta\alpha_i)^2\right]\left[E(\Delta\delta_i^2) - E(\Delta\delta_i)^2\right]} \tag{9}$$

and E( ) denotes average of the quantity in parentheses. The numerical value of the correlation coefficient $\rho$ is a measure of coherence between the two residuals of the angles and lies in the range

$$-1 \leq \rho \leq 1$$

For monotonically related samples, the coefficient of correlation generally gives a good measure of correlation.

B. Results of Analysis

1. The plot of average values of the residuals over each of the 2-hour intervals (see Fig. 13) shows that, over an entire day, the slope is nearly constant, and from day to day, the slopes are nearly equal. The plot further shows that the curves are translated up or down in a random fashion from day to day.

2. The root-mean-square values of the errors over each of the 2-hour intervals computed from Eq. (1) are plotted in Fig. 14 as a function of time.

3. The power spectral-density plots computed from Eq. (3) show that about one half of the noise power is concentrated in the frequency range of from 1/15 to 1/2 cpm for the first 1 1/2 days, and from 1/5 to 1/2 cpm for the remainder of the record. A typical plot is presented in Fig. 15.

4. The autocorrelation function further reveals a harmonic component having a period of approximately 25 min. If it is assumed that this component can be taken out, the autocorrelation function can be represented approximately by an exponential function having a time constant of 50 sec. Figure 16 shows a typical plot.

5. Table 1 is a summary of the correlation coefficient $\rho$, which is computed from Eq. (9), for the 3 days of tracking. It is noted that the linear correlation between the residuals of the declination and the hour angles is less than 10%. A typical plot of the cross-correlation function is presented in Fig. 17.

6. A study of the one-dimensional distribution functions (see Fig. 18 for a typical plot) and autocorrelation functions reveals that the errors in the angular data may be represented by a multivariate Gaussian distribution over each of the 2-hour intervals, or

$$p(y) = \frac{1}{\left[(2\pi)^N \ |M|\right]^{1/2}} \, e^{-1/2 y^T M^{-1} y} \tag{10}$$

where

$$y = \begin{bmatrix} \Delta\delta_1 - E(\Delta\delta_i) \\ \Delta\delta_2 - E(\Delta\delta_i) \\ \cdot \\ \cdot \\ \cdot \\ \Delta\delta_N - E(\Delta\delta_i) \end{bmatrix} = \text{errors} \tag{11}$$

M = moment matrix of the error which is obtained from the autocorrelation function.

For example, M may have the following form for the first two hours of tracking from the second day:

$$M = 10^{-4} \left| \begin{array}{cccccc} 1 & 0.4 & 0.2 & 0.1 & 0 \cdots & 0 \\ 0.4 & 1 & 0.4 & \ddots & \ddots & \ddots \\ 0.2 & 0.4 & 1 & \ddots & \ddots & \ddots \\ 0.1 & \ddots & \ddots & \ddots & \ddots & \ddots \\ 0 & \ddots & \ddots & \ddots & \ddots & \ddots \\ \vdots & & & & & \\ 0 & \ddots & \ddots & \ddots & \ddots & 1 \end{array} \right| \qquad (12)$$

It can be concluded that, from the analysis just described, of the four basic assumptions made with respect to the statistical nature of the data, none are completely justified. Although the errors appear to be normally distributed for data representing relatively short periods of time, a corollary to that assumption is that the data can be made homoscedastic by a proper selection of weighting factors.

The weighting factors which were used for PIONEER IV were those determined a priori from calibrated characteristics of the tracking stations. It is evident, however, that the deterioration in data expected from preflight calibrations did not correspond exactly to that observed in PIONEER IV. The weighting factors used were expressed as polynomials in range and elevation angle from the stations in question. The coefficients in the polynomial were, however, unfortunately different in flight than had been predicted.

Although it is evident that data sampled at the rate of one every 10 sec are correlated in time, during the flight of PIONEER IV, the least-squares fitting routines were applied to samples generally of not more than 1-min frequency. Thus, for the relatively slow data rates actually used, time correlation was apparently not a major problem.

Table 1 shows that a correlation actually did exist between the errors in declination angles and hour angles. However, the relatively small correlation factor of one tenth apparently did not affect the assumptions made.

The assumption of constancy of bias appears to have been violated in two major ways. On any one of the tracking days, the bias appears to be representable by a constant plus a term which varies approximately linearly with hour angle. Preflight calibration of the Goldstone antenna, made by observing stars at various declinations through the boresight telescope, also shows angular errors which vary with local hour angle. As the biases must, in part, be the result of deflections in the dish structure, errors in the biases with respect to preflight calibrations may be the result of relative deflections between the RF and optical axes. The RF and optical axes are aligned using a collimation tower approximately 1 mile from the Goldstone dish. A further calibration of the RF axis is accomplished by tracking a helicopter-borne RF and optical target by means of the primary antenna and a precision optical theodolite.

The hour-angle dependent bias appears to be the result, in part, of dimensional discrepancies in the encoding system, which will be removed by an improved position pick off system. The dependent bias appears to be repeatable from day to day and amenable to preflight calibration.

The reason for the day-to-day variation of the numerically much larger constant-bias term is not presently known. The uncertainty in the determination of the magnitude of the constant bias using the tracking program during the flight of PIONEER IV is estimated to have been of the order of 1 minute of arc.

In order to improve the reduction to homoscedasticity and facilitate the handling of ever greater quantities of tracking data, special data-handling techniques are presently being programmed for the computer. It is hoped that, in the future, all tracking data transmitted from the stations will be stored directly in the computer; that is, be independent of tape-to-card conversion.

In the simplest method of data compression presently being programmed, specified sub-sets of the total data stored can be selected and inserted into the tracking program. A second data-compression method, which utilizes least-mean-square polynomial fits to the raw data over predetermined time intervals, is used to insert one smoothed point per interval, as well as the standard deviation over that interval, into the orbit-determination program. The degree of the polynomials used and the intervals taken are determined, prior to flight, by matching the standard trajectory. The lower bound on length of time interval used is determined by the lowest expected noise frequency. For example, for PIONEER IV, a second- or a third-degree polynomial would require time intervals greater than 11 or 22 min, respectively, as the lowest undesired frequency component was 1/22 cpm.

The third and most complex method of data compression presently being programmed also makes use of least-squares-fit polynomials to sections of the raw data. However, in this case, the polynomials used are determined by first fitting to the current best estimate of the flight trajectory, and then determining the constant of translation of this polynomial necessary to optimize the fit with respect to the raw data.

It is evident that, in the first of the three methods of data compression, a maximum amount of information is discarded for a specified rate of data insertion into the standard tracking program. Although the third method extracts a relatively large amount of information from the data received, it represents a significant complication in the machine computing program. It is not yet clear which method of data compression will yield the best results for a specified machine computing time.

The standard deviations obtained by polynomial fitting data-compression routines can be used to produce an essentially homoscedastic set. The standard deviation required to give the property correct relative weighting between data of various types and from various sources can be obtained in two ways: (1) It is assumed that the quality of a set of data is inversely related to its noise content. (2) It is assumed that the quality of the data is inversely related to the deviation of a set of points of one type from one station from the mean of all types of data from all stations.

It should be noted that, for PIONEER III, the noise standard deviation was used for the raw data weighting and for PIONEER IV the standard deviation from the mean was used as a relative weighting. It is evident that occasions may arise when neither of these standard deviations should be used. In the first method, if the data is smooth but biased, it is weighted too heavily. The second method represents the majority rule, which is not always right.

In order to minimize the expected difficulties with the relative weighting method used during PIONEER IV, a special sub-routine was provided which, on command by means of a sense switch, would change all relative weightings to unity. Thus, if during the tracking procedure, one data type is erroneously completely misfitted, such that its standard deviation from the mean is much larger than all the other data types, the least-squares fitting routine will only slowly converge to include the misfitted data type. In order to accelerate this convergence, the reduction of the relative weighting to unity is used for one or two iterations and then removed to complete the convergence using the proper relative weighting. It should be noted that close agreement between the standard deviations from the mean and the noise standard deviations obtained by fitting separately to each data type is a good indication of convergence of the iteration process.

The most serious unresolved problem in the tracking program is a proper determination of the degree of degeneracy of the matrix involved in the solution for the changes in initial conditions. Such degeneracy occurs either because of inadequacies in the calculation of the partial derivatives or a partial or complete degeneracy in the tracking geometry. It is evident that both of these sources of difficulties are related in the sense that it is more difficult to compute partial derivatives when the tracking geometry becomes weak or degenerate. For example, with the probe far from the center of the Earth, angle data alone cannot be used to compute distance from the station. Similarly, range rate or range data cannot be used to compute the angular position.

During PIONEER IV, difficulties with degenerate matrices were avoided primarily by applying the experience gained during preflight practice runs on the computer using simulated tracking data. In the procedure evolved during these practice runs, the order of the matrix used varied from three to eight as a function of quality and quantity of data. During the early part of the flight, when the data was primarily that from Puerto Rico, the maximum number of initial conditions solved for at any one time was three. The particular set of coordinates used was alternated essentially between the position and velocity coordinates. During the later portions of the flight, when substantial quantities of Goldstone data were available, the changes in all six of the initial conditions could be solved for in addition to two of the biases.

With the increasingly complex geometries and the increasing quantities of data to be expected in future flights, analytical procedures must be made available for determining the size of the largest non-degenerate matrix. It is in this area that the present tracking program has its greatest weakness and would most benefit from improvement of the program.

Table 1. Correlation Coefficients and Expected Values

| Day | $E\left[\Delta\alpha_i\right]$ | $E\left[\Delta\delta_i\right]$ | $E\left[\Delta\alpha_i \cdot \Delta\delta_i\right]^{1/2}$ | $E\left[\Delta\alpha_i^2\right]^{1/2}$ | $E\left[\Delta\delta_i^2\right]^{1/2}$ | $\rho$ |
|---|---|---|---|---|---|---|
| 1 | -0.00187 | -0.0103 | 0.0051 | 0.0086 | 0.0140 | 0.086 |
| 2 | -0.00182 | 0.0098 | 0.0040 | 0.0117 | 0.0182 | -0.012 |
| 3 | -0.0021 | -0.0093 | 0.0069 | 0.0170 | 0.0170 | 0.068 |

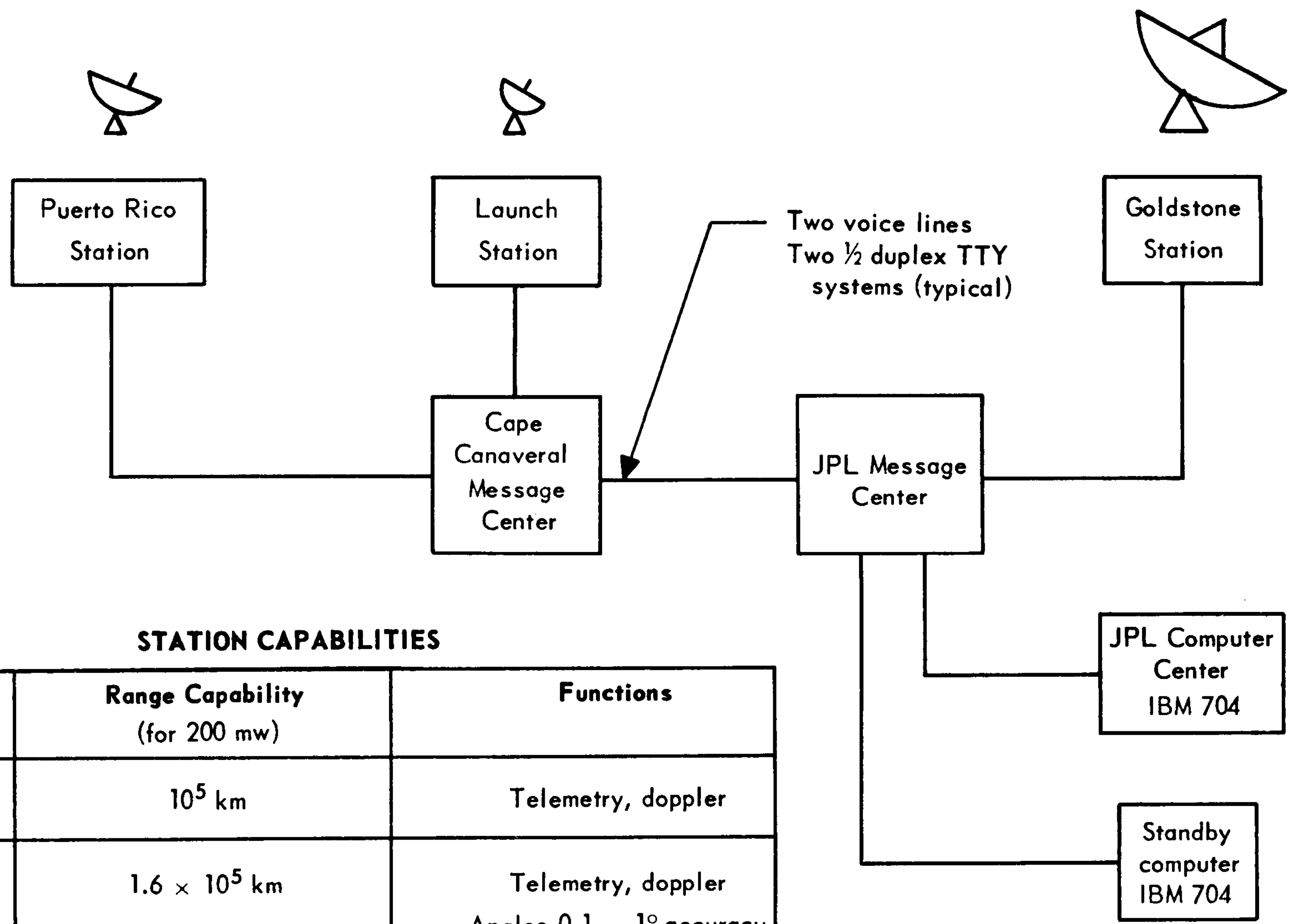


**STATION CAPABILITIES**

| Station | Range Capability (for 200 mw) | Functions |
|---|---|---|
| Launch | $10^5$ km | Telemetry, doppler |
| Puerto Rico | $1.6 \times 10^5$ km | Telemetry, doppler<br>Angles 0.1 – 1° accuracy |
| Goldstone | $1.8 \times 10^6$ km | Telemetry, doppler<br>Angles .01 – .1 accuracy |

Fig. 1. Basic Tracking Network for PIONEERS III and IV

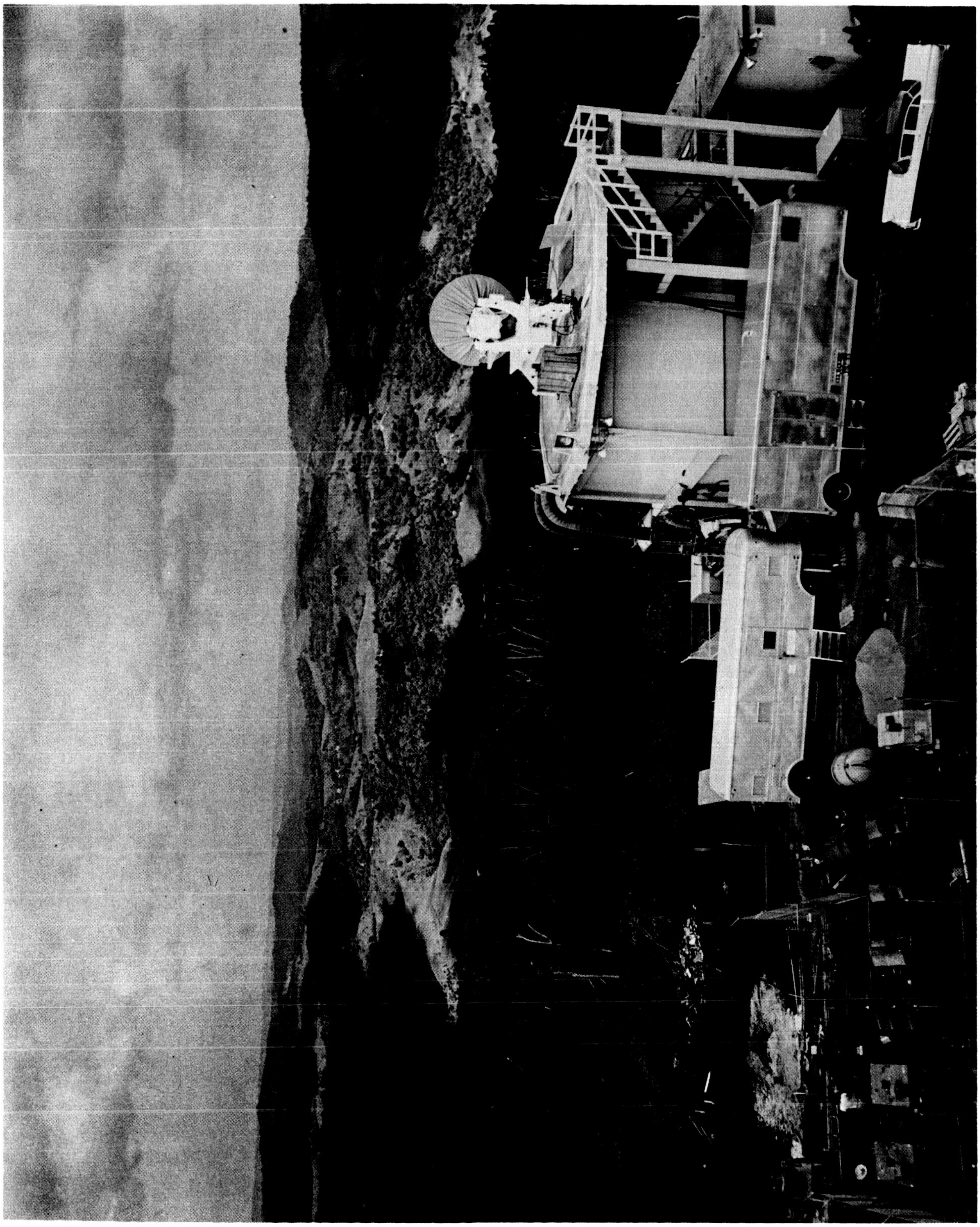

Fig. 2. Puerto Rico Downrange Tracking Station

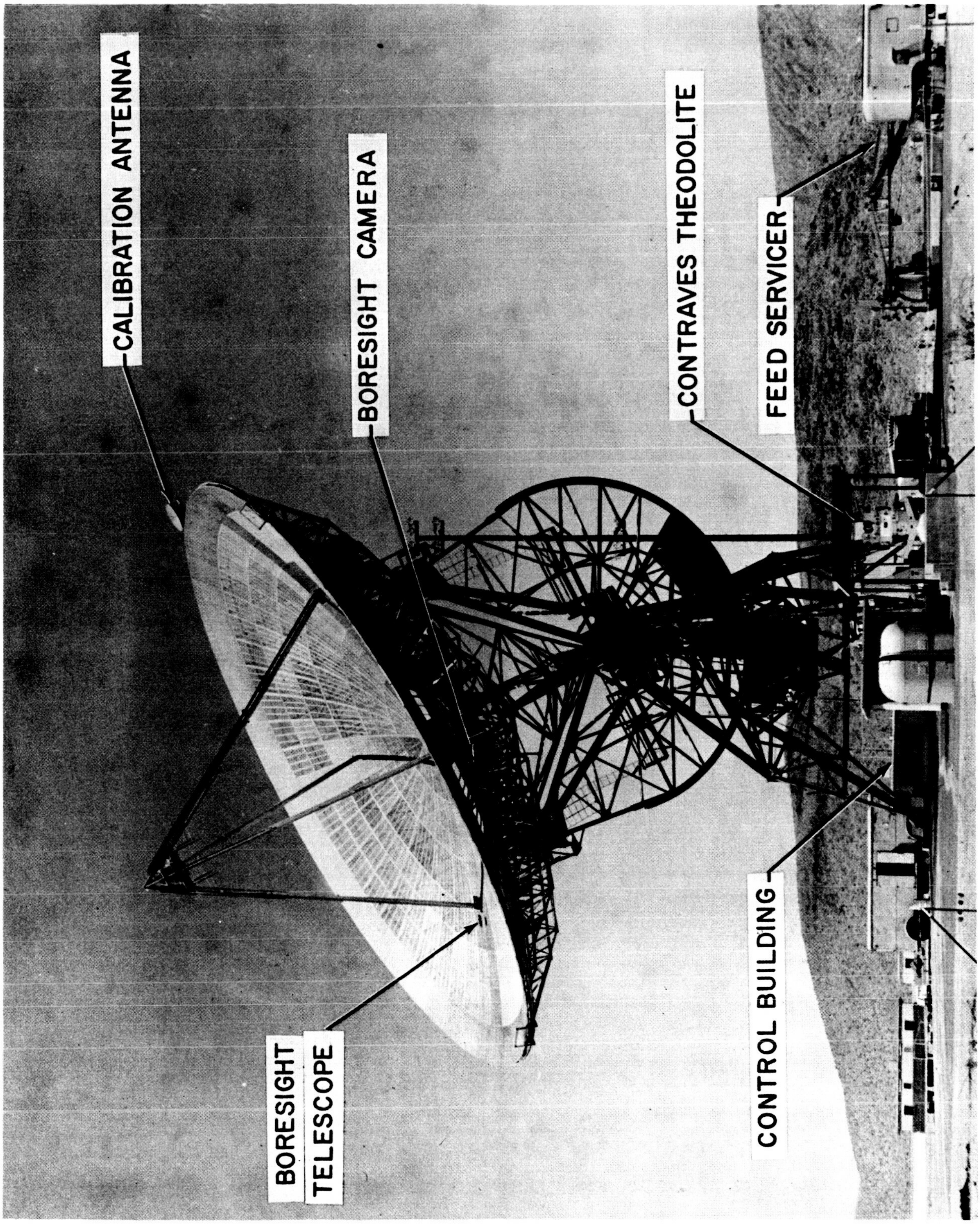


Fig. 3. Goldstone Lake Tracking Station

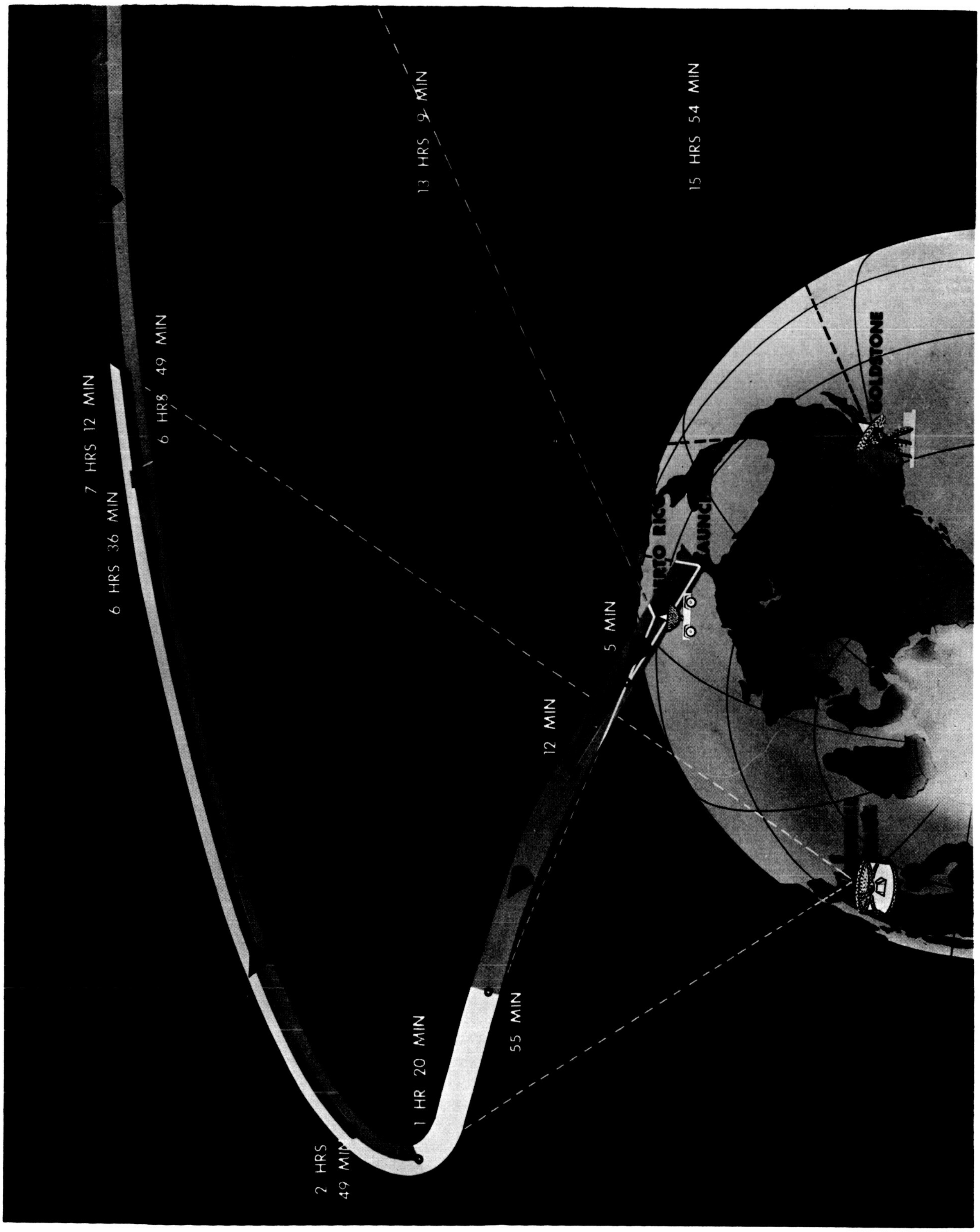


Fig. 4. Initial Path of PIONEER Moon Probe (Earth Fixed)

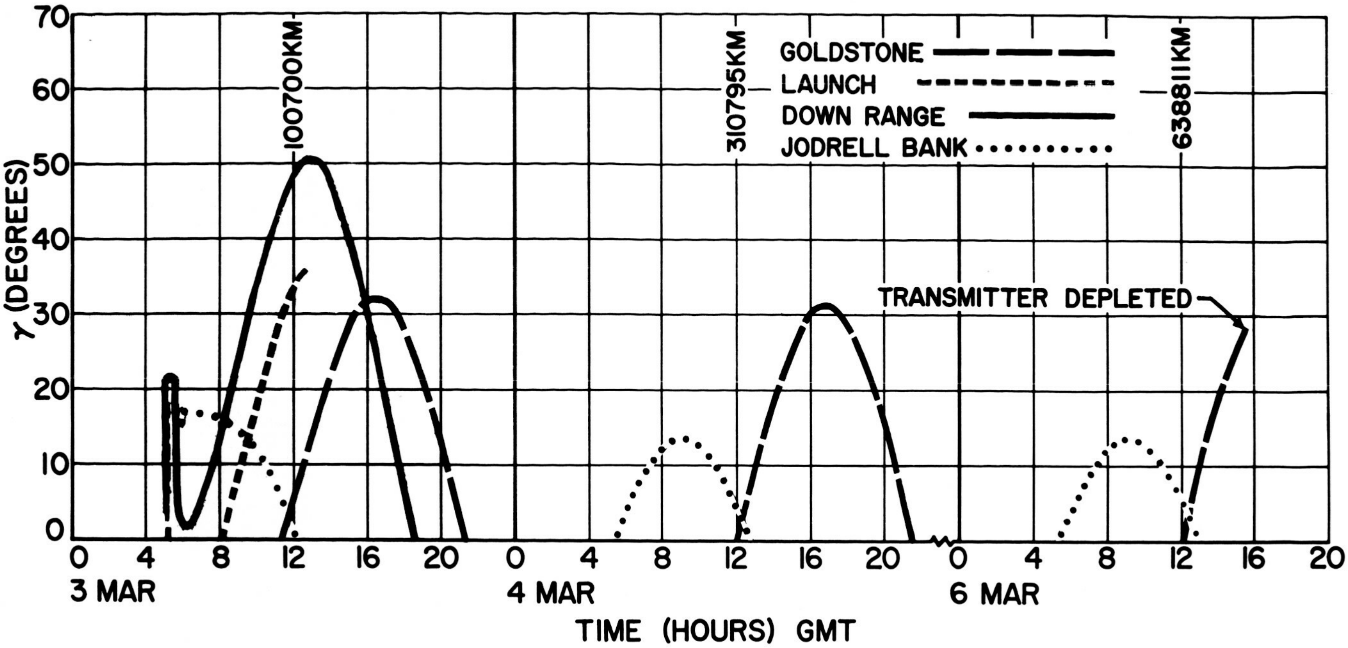


Fig. 5. Plot of Elevation Angle vs Time for PIONEER IV

Fig. 6. PIONEER III and IV Computing Center

| STATION IDENTIFICATION | DATA CONDITION | GMT IN HOURS, MINUTES, SECONDS | GOLDSTONE HOUR ANGLE IN THOUSANDTHS DEGREES | GOLDSTONE DECLINATION ANGLE IN THOUSANDTHS DEGREES | COUNTED DOPPLER FREQUENCY IN CYCLES PER SECOND |
|---|---|---|---|---|---|
| 2 | Ø | 1514Ø1 | 335476 | 336524 | 11337 |
| 2 | Ø | 151411 | 3355Ø8 | 336524 | 11336 |
| 2 | Ø | 151421 | 335556 | 336524 | 11336 |
| 2 | Ø | 151431 | 335648 | 336524 | 11337 |
| 2 | Ø | 151441 | 335736 | 336524 | 11338 |
| 2 | Ø | 151451 | 33582Ø | 336524 | 11336 |
| 2 | Ø | 1515Ø1 | 335848 | 336524 | 11337 |

Fig. 7. Sample of Goldstone Data Message

Fig. 8. Data Handling Facility

| GMT IN HOURS, MINUTES, SECONDS | GOLDSTONE HOUR ANGLE IN THOUSANDTHS DEGREES | GOLDSTONE DECLINATION ANGLE IN THOUSANDTHS DEGREES | COUNTED DOPPLER FREQUENCY IN CYCLES PER SECOND | GOLDSTONE HOUR ANGLE RATE IN THOUSANDTHS DEGREES PER HOUR | GOLDSTONE DECLINATION ANGLE RATE IN THOUSANDTHS DEGREES PER HOUR | RANGE IN KILOMETERS |
|---|---|---|---|---|---|---|
| 131201 | 304776 | 336507 | 11329 | 015102 | -00048 | 492858 |
| 131301 | 305027 | 336506 | 11329 | 015102 | -00048 | 492954 |
| 131401 | 305277 | 336504 | 11329 | 015103 | -00048 | 493050 |
| 131601 | 305779 | 336501 | 11329 | 015104 | -00048 | 493242 |
| 131701 | 306029 | 336500 | 11329 | 015105 | -00048 | 493338 |
| 131801 | 306280 | 336498 | 11329 | 015105 | -00047 | 493435 |
| 131901 | 306531 | 336497 | 11329 | 015106 | -00047 | 493531 |

Fig. 9. Sample of Goldstone Acquisition Message

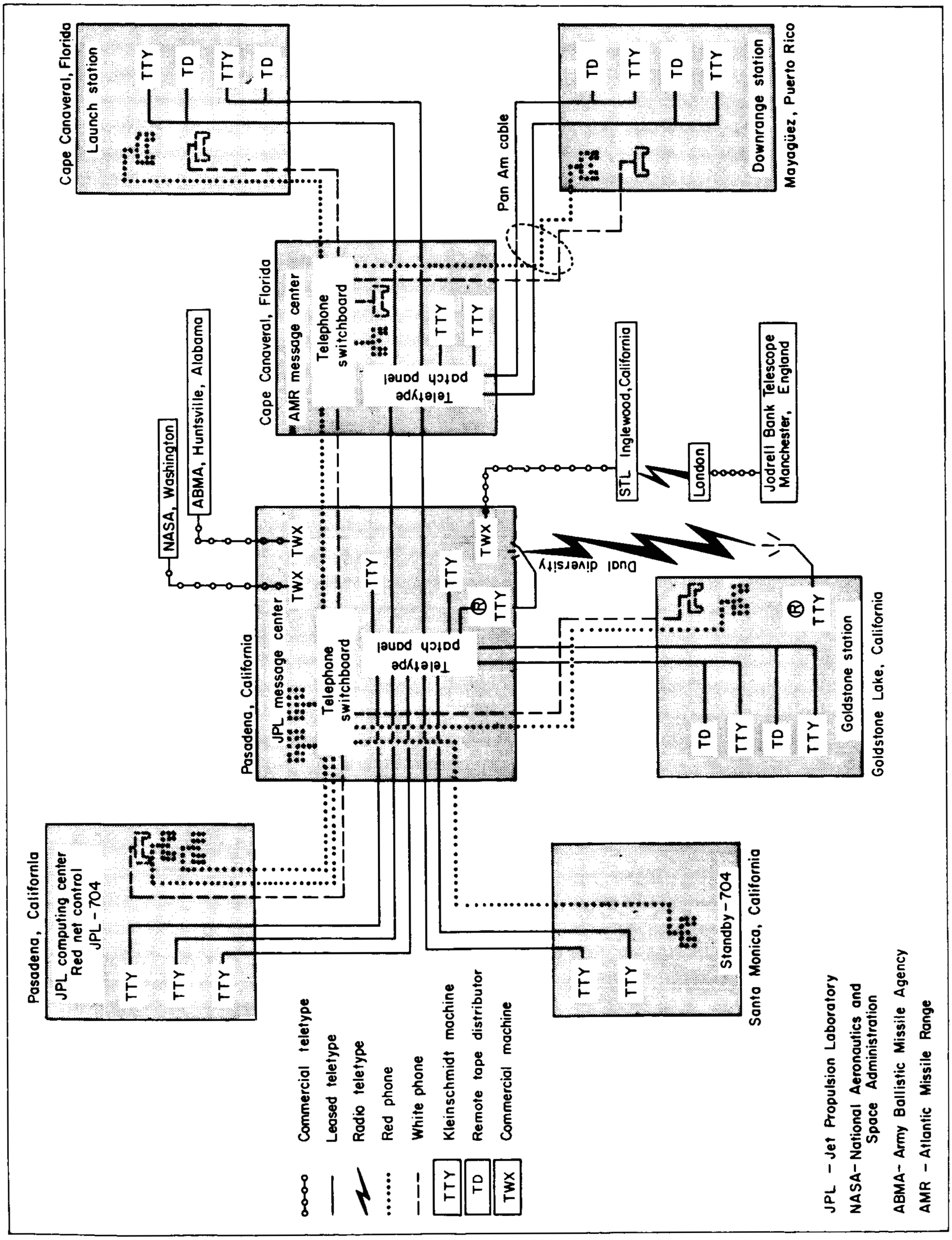


Fig. 10. PIONEER III and IV Communications Network

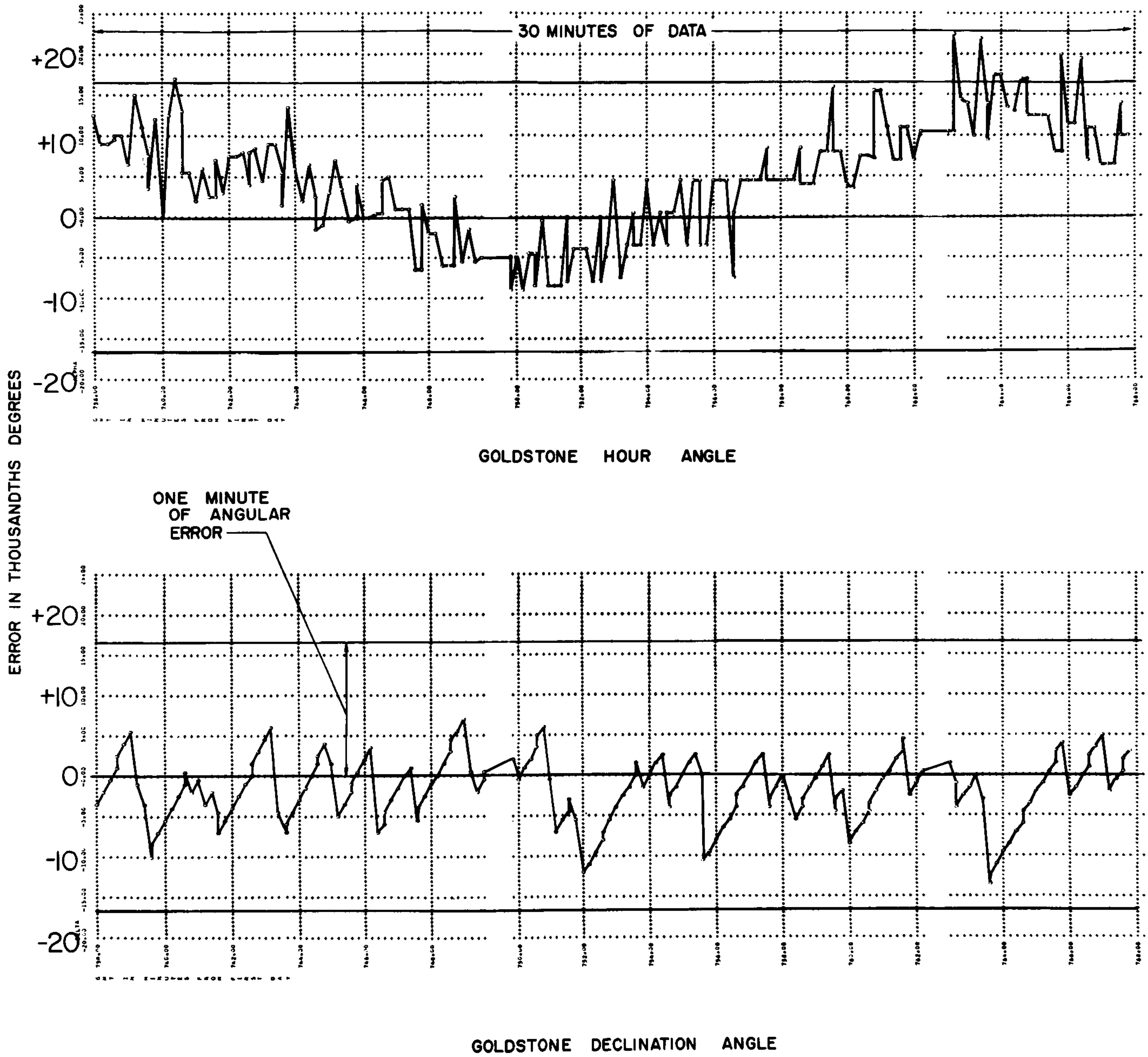


Fig. 11. Goldstone Angular Errors (100, 000-km Range)

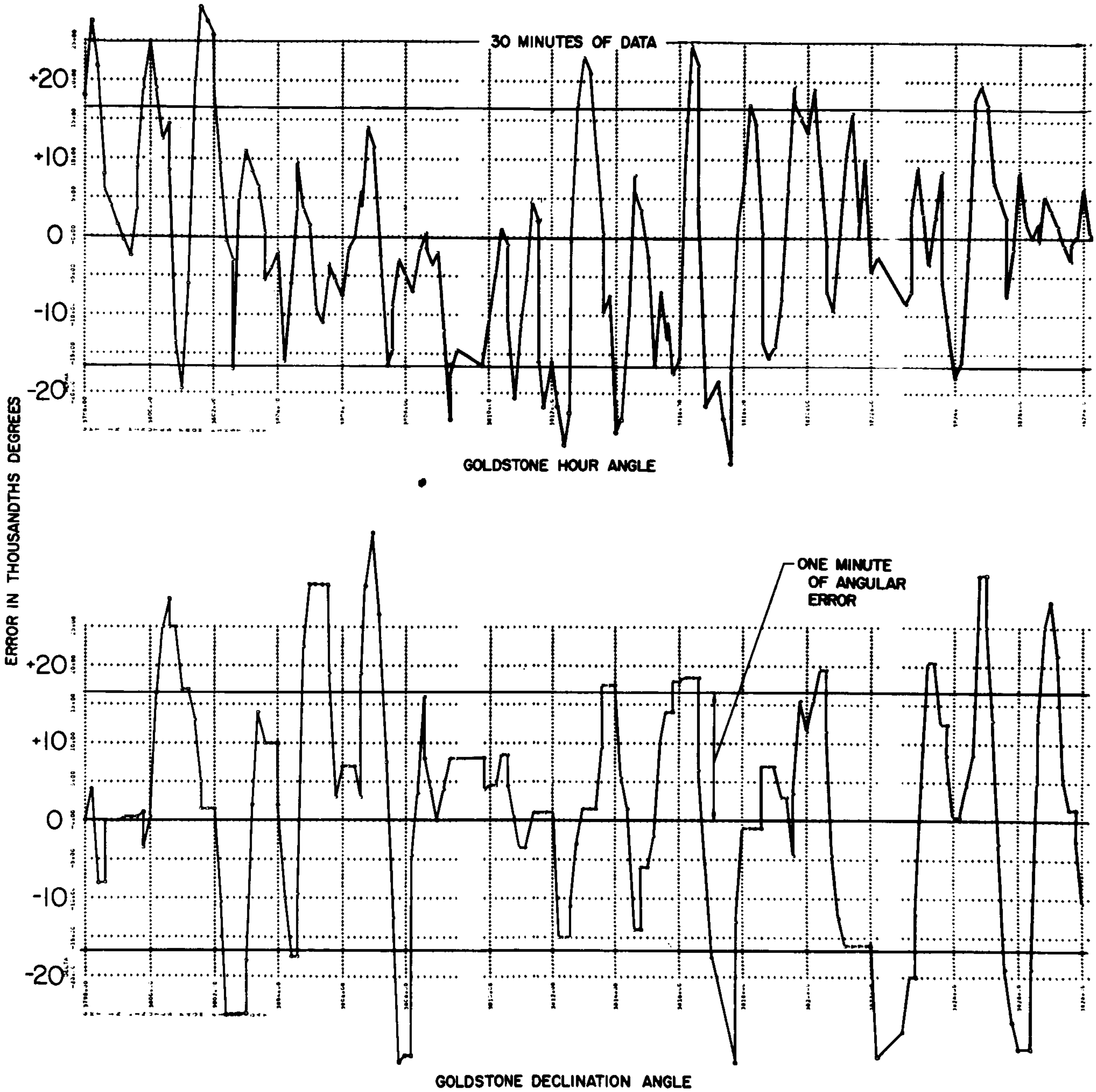


Fig. 12. Goldstone Angular Errors (500,000-km Range)

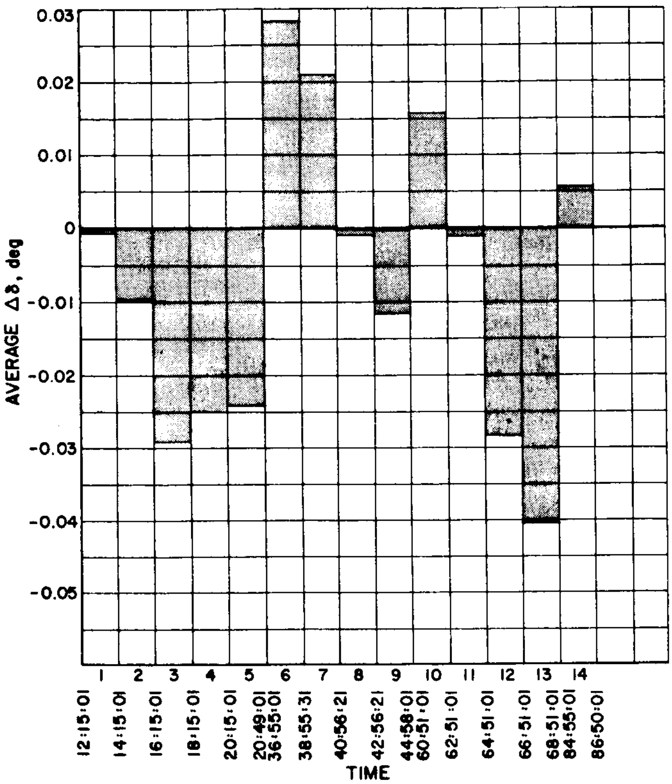


Fig. 13. Goldstone Δδ Average over 2-Hour Intervals

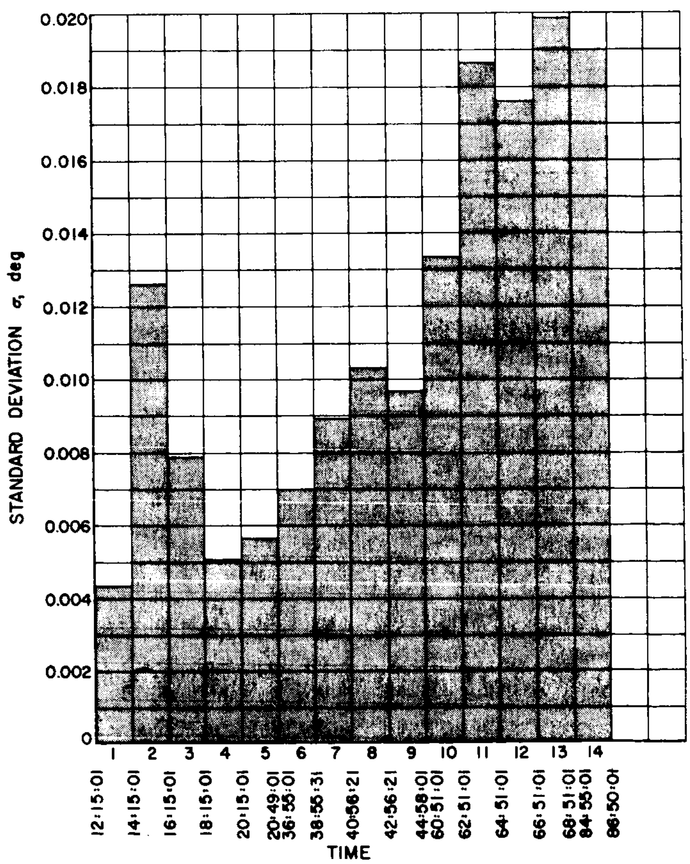


Fig. 14. Goldstone Δδ Standard Deviation

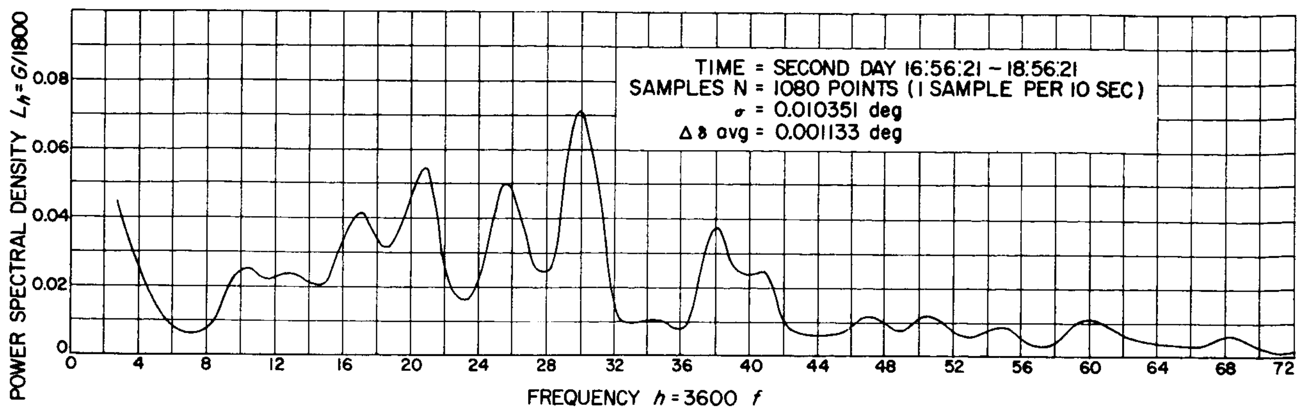


Fig. 15. Goldstone Δδ Normalized Power Spectral Density

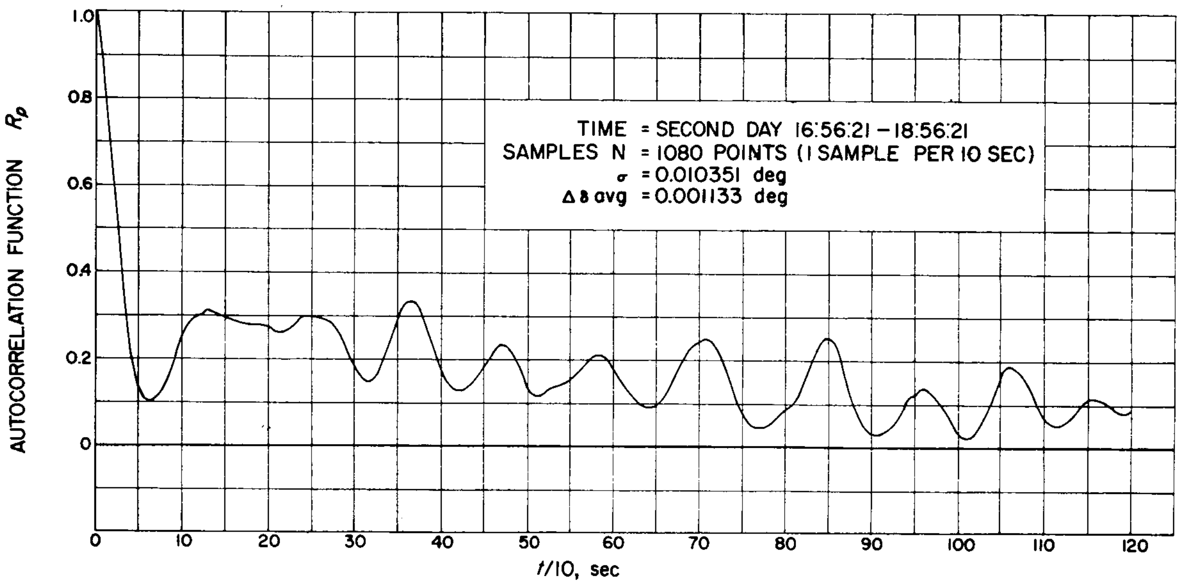


Fig. 16. Goldstone Δδ Normalized Autocorrelation Function

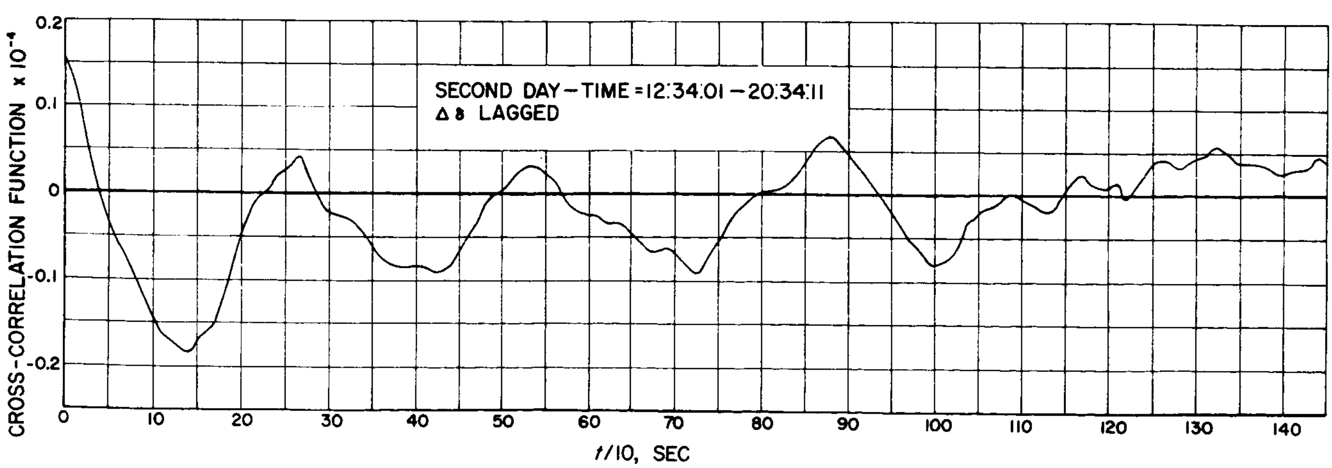


Fig. 17. Cross-Correlation Between Δα and Δδ PIONEER IV Data from Goldstone

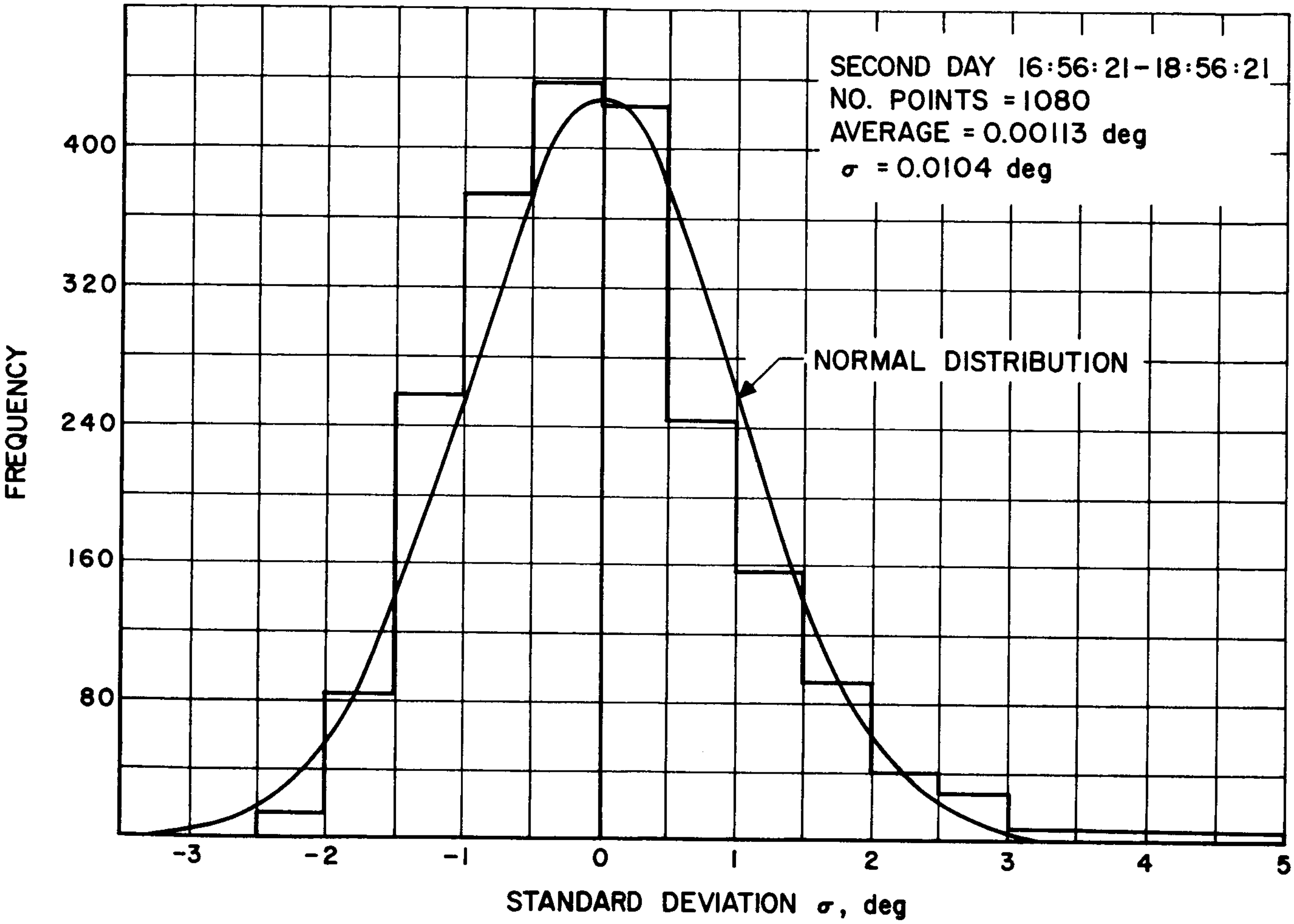


Fig. 18. Normalized Distribution-Goldstone